



ELSEVIER

Available online at www.sciencedirect.com

SCIENCE @ DIRECT®

Optics Communications 223 (2003) 221–232

OPTICS
COMMUNICATIONS

www.elsevier.com/locate/optcom

Analysis of evanescent waves conversion by a non-spherical particle near a metal-coated glass prism via discrete sources method

Yuri Eremin^a, Thomas Wriedt^{b,*}

^a Faculty of Applied Mathematics and Computer Science, Moscow State University, Lenin's Hills, 119992 Moscow, Russia

^b Institut für Werkstofftechnik, Badgasteiner Str. 3, 28359 Bremen, Germany

Received 27 February 2003; received in revised form 25 June 2003; accepted 26 June 2003

Abstract

The discrete sources method is extended to analyse evanescent waves scattering by a non-spherical particle located near a metal-coated glass prism. A metallic film is designed to enhance conversion of an evanescent wave into a scattered one via computational simulations. The importance of taking into account interaction between scatterer and multi-layered interface is demonstrated.

© 2003 Elsevier B.V. All rights reserved.

PACS: 42.25.B

Keywords: Scattering microscopy; Evanescent waves; Discrete sources method

1. Introduction

The problem of reconstruction of a scattering object has been extensively studied in the last decades. Evanescent wave microscopy seems to be especially useful for reconstruction of nano-structures [1,2]. Evanescent wave microscopy provides a high contrast image with sub-wavelength resolution. Employing evanescent waves scattering in combination with surface plasmon resonance in the vicinity of a metal-coated glass surface leads to image magnification [3,4]. The wide potential of application of scattering microscopy especially in biology, materials science and information technology gives rise to renewed interest in computer simulation of scattering of evanescent waves by a particle located near a metal-coated dielectric prism surface. Earlier, scattering by particles was mainly analysed using approximate models. One of the most widespread models is based on the Mie theory extended to the evanescent waves scattering [4,5].

* Corresponding author. Tel.: +494212182507; fax: +494212185378.

E-mail addresses: eremin@cs.msu.su (Y. Eremin), thw@iwt.uni-bremen.de (T. Wriedt).

Such approach as a rule does not accurately take into account particle-surface scattering interaction. In recent papers by Doicu et al. [6,7] a computer model for the evanescent wave scattering analysis was developed based on the discrete sources method. The model takes into account complete scatterer–prism interaction and provides an opportunity to investigate evanescent wave scattering by any axial symmetric scatterer. It has been demonstrated that only a rigorous model can adequately describe scattering of evanescent waves by a particle located near a plane surface [6].

In the present paper the discrete sources method (DSM) is extended to the analysis of evanescent waves scattering by a non-spherical particle located near a multi-layered interface. We investigate the conversion of an evanescent wave into scattered wave by a small penetrable particle deposited near a metal-coated glass prism. Using computer simulations, we treat the problem of optimal design of a metallic film and optimal choice of the incident angle providing the maximum enhancement of the scattered intensity in a certain solid angle.

2. Discrete sources method

In this section the DSM applied to the analysis of evanescent wave scattering is briefly described. We start with the mathematical statement of the scattering problem. Let us consider an axial symmetric penetrable particle with interior domain D_i and smooth boundary S deposited above the plane surface Σ_f of a metallic film (Fig. 1). The film of thickness d occupying domain D_f is located on a planar surface Σ_1 of a glass prism. We denote the prism domain by D_1 and ambient domain exterior to the particle by D_0 . Let us introduce Cartesian coordinate system $Oxyz$ by choosing its origin O at the intersection point of the axis of symmetry and the plane Σ_1 . The z -axis coincides with the axis of symmetry and is directed into domain D_0 . So that the $z = 0$ and $z = d$ planes coincide with the Σ_1 and Σ_f planes, respectively. We assume that exciting field $\{\mathbf{E}_1^i, \mathbf{H}_1^i\}$ is a linear polarized plane wave propagating from the glass prism at angle β_1 with respect to the z -axis. According to the Snell's law wave $\{\mathbf{E}_0^i, \mathbf{H}_0^i\}$ refracted in D_0 propagates at angle β_0 to the z -axis. Then the mathematical statement of the scattering problem can be formulated in the following form:

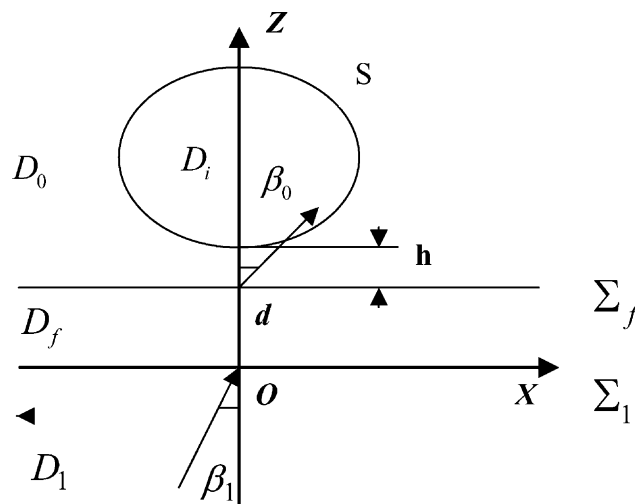


Fig. 1. Model geometry of particle positioned on metal-coated glass surface.

$$\begin{aligned}
 \nabla \times \mathbf{H}_\zeta &= jk\varepsilon_\zeta \mathbf{E}_\zeta; & \nabla \times \mathbf{E}_\zeta &= -jk\mu_\zeta \mathbf{H}_\zeta & \text{in } D_\zeta, \zeta = 0, f, 1, i, \\
 \mathbf{n} \times (\mathbf{E}_i - \mathbf{E}_0) &= 0, & \mathbf{n} \times (\mathbf{H}_i - \mathbf{H}_0) &= 0 & \text{on } S, \\
 \mathbf{e}_z \times (\mathbf{E}_0 - \mathbf{E}_f) &= 0, & \mathbf{e}_z \times (\mathbf{H}_0 - \mathbf{H}_f) &= 0 & \text{on } \Sigma_f, \\
 \mathbf{e}_z \times (\mathbf{E}_f - \mathbf{E}_1) &= 0, & \mathbf{e}_z \times (\mathbf{H}_f - \mathbf{H}_1) &= 0 & \text{on } \Sigma_1,
 \end{aligned}
 \tag{1}$$

and radiation (attenuation) conditions at infinity.

Here, \mathbf{n} is the outward unit normal vector to S , $k = \omega/c$ and $\{\mathbf{E}_\zeta, \mathbf{H}_\zeta\}$ stands for the total field in corresponding domain D_ζ . Note that the total field in D_0 is a superposition of the refracted exciting field and the scattered one, that is $\mathbf{E}_0 = \mathbf{E}_0^s + \mathbf{E}_0^i$, $\mathbf{H}_0 = \mathbf{H}_0^s + \mathbf{H}_0^i$. If $\text{Im } \varepsilon_\zeta, \mu_\zeta \leq 0$ (time dependence for the fields is chosen as $\exp\{j\omega t\}$) and the particle surface is smooth enough $S \subset C^{(1,\alpha)}$, then the above boundary-value problem is uniquely solvable.

We construct an approximate solution to the scattering problem (1) via the DSM by representing the electromagnetic fields as a finite linear combination of the fields of dipoles and multipoles [8]. The approximate solution satisfies the Maxwell equations in domains $D_\zeta, \zeta = 0, f, 1$, infinity conditions and the transmission conditions at the plane interfaces $\Sigma_{f,1}$. Eventually, the scattering problem is reduced to the problem of approximating the exciting field on particle surface S . The amplitudes of discrete sources are determined from the boundary conditions at the particle surface, which can be rewritten as

$$\mathbf{n} \times (\mathbf{E}_i - \mathbf{E}_0^s) = \mathbf{n} \times \mathbf{E}_0^i, \quad \mathbf{n} \times (\mathbf{H}_i - \mathbf{H}_0^s) = \mathbf{n} \times \mathbf{H}_0^i \quad \text{on } S.
 \tag{2}$$

To satisfy the transmission conditions analytically at the plane interfaces $\Sigma_{f,1}$ we use the Green’s tensor for a stratified interface

$$\overleftrightarrow{\mathbf{G}}(\mathbf{r}, \mathbf{r}_0) = \begin{bmatrix} \mathbf{g}^{e,h} & 0 & 0 \\ 0 & \mathbf{g}^{e,h} & 0 \\ \frac{\partial f}{\partial x} & \frac{\partial f}{\partial y} & \mathbf{g}^{h,e} \end{bmatrix}.
 \tag{3}$$

An approximate solution to the scattering problem is constructed fulfilling analytically the transmission conditions on plane interfaces $\Sigma_{f,1}$ and taking into account the rotational symmetry of the scattering problem geometry and polarisation of the exciting field [8].

First, let us consider a P -polarized exciting field. In this case, the refracted plane wave in D_0 accepts the following form:

$$\mathbf{E}_0^i(\mathbf{r}) = T^P(-\mathbf{e}_x \cos \beta_0 + \mathbf{e}_z \sin \beta_0) \exp\{-jk_0(x \sin \beta_0 + z \cos \beta_0)\},
 \tag{4}$$

$$\mathbf{H}_0^i(\mathbf{r}) = -T^P n_0 \mathbf{e}_y \exp\{-jk_0(x \sin \beta_0 + z \cos \beta_0)\},$$

where $(\mathbf{e}_x, \mathbf{e}_y, \mathbf{e}_z)$ are unit vectors of the Cartesian coordinate system and T^P is the transmission coefficient corresponding to a multi-layered interface for P -polarization

$$T^P = \frac{T_{1f}^P T_{f0}^P \exp(ik_f \cos \beta_f d)}{1 + R_{1f}^P R_{f0}^P \exp(2ik_f \cos \beta_f d)},
 \tag{5}$$

here $k_\zeta = k\sqrt{\varepsilon_\zeta \mu_\zeta}$, $\zeta = 0, f, 1$; β_ζ is refractive angle inside D_ζ , $\zeta = 0, f, 1$,

$$T_{\tau l}^P = \frac{2n_\tau \cos \beta_\tau}{n_\tau \cos \beta_l + n_l \cos \beta_\tau}$$

and

$$R_{\tau l}^P = \frac{n_\tau \cos \beta_l - n_l \cos \beta_\tau}{n_\tau \cos \beta_l + n_l \cos \beta_\tau},$$

are the transmission and reflection Fresnel coefficients associated with interfaces $\Sigma_{f,1}$ for the P -polarization [9]. If $\beta_1 > \arcsin(n_0/n_1)$ the exciting wave is totally reflected from plane Σ_f and only an evanescent wave travelling along surface Σ_f and damped in the \mathbf{e}_z direction is present in D_0 . It follows from the Snell's law that in this case: hence, $\cos \beta_0$ becomes purely imaginary. We choose the value

$$\cos \beta_0 = -j\sqrt{\sin^2 \beta_0 - 1},$$

since otherwise the amplitude of the refracted wave would tend to infinity with the increasing distance.

As mentioned above, the approximate solution to the scattering problem is constructed by taking into account not only the rotational symmetry of the scattering problem geometry, but also the polarization of the external excitation [8]. In this context, for P -polarized exciting plane wave (4) we use the following electric and magnetic vector potentials:

$$\begin{aligned} \mathbf{A}_{mn}^{e,0}(\mathbf{r}) &= \{g_m^e(\eta, z_n) \cos(m+1)\varphi; -g_m^e(\eta, z_n) \sin(m+1)\varphi; -f_{m+1}(\eta, z_n) \cos(m+1)\varphi\}, \\ \mathbf{A}_{mn}^{h,0}(\mathbf{r}) &= \{g_m^h(\eta, z_n) \sin(m+1)\varphi; g_m^h(\eta, z_n) \cos(m+1)\varphi; -f_{m+1}(\eta, z_n) \sin(m+1)\varphi\}, \\ \mathbf{A}_{0n}^{e,h,0}(\mathbf{r}) &= \{0; 0; g_0^{h,e}(\eta, z_n)\}, \end{aligned} \tag{6}$$

where $g_m^{e,h}, f_m$ are the Fourier harmonics corresponding to the Green tensor components, which accept the following form:

$$g_m^{e,h}(\eta, z_n) = \int_0^\infty J_m(\lambda\rho) v_{11}^{e,h}(z, z_n, \lambda) \lambda^{1+m} d\lambda, \quad f_m(\eta, z_n) = \int_0^\infty J_m(\lambda\rho) v_{31}(z, z_n, \lambda) \lambda^{1+m} d\lambda. \tag{7}$$

Here J_m is the cylindrical Bessel function, (ρ, φ, z) are the cylindrical coordinates, $\eta = (\rho, z)$, $R_{\eta z_n}^2 = \rho^2 + (z - z_n)^2$, while $\{z_n\}_{n=1}^\infty$ is a dense set of source points distributed over a segment $\Gamma_z^0 \in D_i$ of the axis of symmetry, and $v_{11}^{e,h}(z, z_n, \lambda)$, $v_{31}(z, z_n, \lambda)$ are the corresponding spectral functions. The spectral functions provide the continuity of the field tangential components on the interfaces $\Sigma_{f,1}$ can be represented as follows:

$$\begin{aligned} v_{11}^{e,h} &= \begin{cases} \frac{\exp\{-\eta_0|z-z_n|\}}{\eta_0} + A_{11}^{e,h}(\lambda, z_n) \exp\{-\eta_0|z-d|\}, & z \geq d, z_n > 0, \\ B_{11}^{e,h}(\lambda, z_n) \exp\{-\eta_f|z-d|\} + C_{11}^{e,h}(\lambda, z_n) \exp\{-\eta_f z\}, & d \geq z \geq 0, \\ D_{11}^{e,h}(\lambda, z_n) \exp\{\eta_1 z\}, & z \leq 0, \end{cases} \\ v_{31}^{e,h} &= \begin{cases} A_{31}^{e,h}(\lambda, z_n) \exp\{-\eta_0|z-d|\}, & z \geq d, z_n > 0, \\ B_{31}^{e,h}(\lambda, z_n) \exp\{-\eta_f|z-d|\} + C_{31}^{e,h}(\lambda, z_n) \exp\{-\eta_f z\}, & d \geq z \geq 0, \\ D_{31}^{e,h}(\lambda, z_n) \exp\{\eta_1 z\}, & z \leq 0, \end{cases} \end{aligned}$$

where $\eta_\zeta^2 = \lambda^2 - k_\zeta^2$, $\zeta = 0, f, 1$. Spectral coefficients A, B, C and D can be determined from the transmission conditions on plane interfaces $\Sigma_{f,1}$ which have the form [8]

$$\begin{aligned} [v_{11}^e] &= \left[\frac{1}{\mu} \frac{\partial v_{11}^e}{\partial z} \right] = 0, \quad [v_{11}^h] = \left[\frac{1}{\varepsilon} \frac{\partial v_{11}^h}{\partial z} \right] = 0, \\ \left[\frac{1}{\mu} v_{31}^e \right] &= 0, \quad \left[\frac{1}{\varepsilon\mu} \frac{\partial v_{31}^e}{\partial z} \right] = \left[\frac{1}{\varepsilon\mu} \right] v_{11}^e, \quad \left[\frac{1}{\varepsilon} v_{31}^h \right] = 0, \quad \left[\frac{1}{\varepsilon\mu} \frac{\partial v_{31}^h}{\partial z} \right] = \left[\frac{1}{\varepsilon\mu} \right] v_{11}^h. \end{aligned}$$

In particular, the equality $v_{31}^e = v_{31}^h$ holds at $z \geq d$.

For the total field inside particle D_i we determine the following vector potentials [8]

$$\begin{aligned} \mathbf{A}_{mn}^{e,i}(\mathbf{r}) &= \{J_m^i(\eta, z_n) \cos(m+1)\varphi; -J_m^i(\eta, z_n) \sin(m+1)\varphi; 0\}, \\ \mathbf{A}_{mn}^{h,i}(\mathbf{r}) &= \{J_m^i(\eta, z_n) \sin(m+1)\varphi; J_m^i(\eta, z_n) \cos(m+1)\varphi; 0\}, \\ \mathbf{A}_{0n}^{e,h,i}(\mathbf{r}) &= \{0; 0; J_0^i(\eta, z_n)\}, \end{aligned} \tag{8}$$

where $J_m^i(\eta, z_n) = j_m(k_i R_{\eta z_n})(\rho/R_{\eta z_n})^m$, $\{z_n\}_{n=1}^\infty$ is a dense set of points distributed over a segment $\Gamma_z^i \in D_i$ of the axis of symmetry and j_m are the spherical Bessel functions. Let us introduce the following notations:

$$\overset{\leftrightarrow}{\mathbf{R}}_1 = \begin{pmatrix} i/k\varepsilon_\zeta\mu_\zeta\nabla \times \nabla \times \\ -1/\mu_\zeta\nabla \times \end{pmatrix}, \quad \overset{\leftrightarrow}{\mathbf{R}}_2 = \begin{pmatrix} 1/\varepsilon_\zeta\nabla \times \\ -i/k\varepsilon_\zeta\mu_\zeta\nabla \times \nabla \times \end{pmatrix}. \quad (9)$$

Now, we can represent the approximate solution to the scattering problem for the P -polarized excitation as

$$\begin{pmatrix} \mathbf{E}_N^\zeta \\ \mathbf{H}_N^\zeta \end{pmatrix} = \sum_{m=0}^M \sum_{n=1}^{N_m^\zeta} \left\{ p_{mn}^\zeta \overset{\leftrightarrow}{\mathbf{R}}_1 \mathbf{A}_{mn}^{e,\zeta} + q_{mn}^\zeta \overset{\leftrightarrow}{\mathbf{R}}_2 \mathbf{A}_{mn}^{h,\zeta} \right\} + \sum_{n=1}^{N_m^\zeta} r_n^\zeta \overset{\leftrightarrow}{\mathbf{R}}_1 \mathbf{A}_n^{e,\zeta}; \quad \zeta = 0, i. \quad (10)$$

The last term in (10) is associated with vertical electric dipoles. Here, N is a complex index incorporating M and N_m^ζ . Let us emphasize that in the DSM, scattered field $\{\mathbf{E}_N^\zeta, \mathbf{H}_N^\zeta\}$ in domains $D_{0,f,1}$ can be represented in terms of the unitary set of amplitudes $\{p_{mn}^0, q_{mn}^0, r_n^0\}$ after the transmission conditions at the interfaces Σ_f and Σ_1 are satisfied using Green’s tensor components (7) [8].

In the same manner scattering of an S -polarized plane wave can be analyzed [8].

The completeness of the system of distributed multipoles used in (10) guarantees the convergence of the approximate solution to the exact solution to (1) in any closed subset of D_0 [10].

As mentioned above representation (10) satisfies all the conditions of scattering problem (1) except the transmission conditions at the particle surface (2). Actually, these conditions are used to determine amplitudes of discrete sources $\{p_{mn}^{0,i}, q_{mn}^{0,i}, r_n^{0,i}\}$. Since the scattering problem geometry is axially symmetric with respect to the Oz -axis and discrete sources are distributed over the axis of symmetry, fulfilling the transmission conditions (2) at surface S can be reduced to the sequential solution of the transmission problems for the Fourier harmonics of the fields. So, instead of matching the fields on the scattering surface (see (2)), we can match their Fourier harmonics thus reducing approximation problem on the surface to a set of the problems enforced on the surface generatrix \mathfrak{S} . By solving these problems one can determine the discrete sources amplitudes $\{p_{mn}^{0,i}, q_{mn}^{0,i}, r_n^{0,i}\}$. Various numerical schemes for determination of the amplitudes are at our disposal. It has been found that stable results can be obtained by using the generalized point-matching technique and pseudo-solution of an over-determined system of linear equations. The DSM is a direct method and hence it allows one to solve the scattering problem for the entire set of incident angles β_1 and both polarizations (P and S) at once. Besides, a new numerical scheme provides an opportunity to control the convergence of the approximate solution by posterior error estimation [8]. After the amplitudes of discrete sources are determined, one can calculate far field pattern $\mathbf{E}_\infty(\theta, \phi)$ of the scattered field, which is determined at the upper part of the unite sphere $\Omega = \{0^\circ \leq \theta < 90^\circ, 0^\circ \leq \phi \leq 360^\circ\}$ and is given by

$$\mathbf{E}_0^s(\mathbf{r})/|\mathbf{E}^0(z=0)| = \frac{\exp\{-ik_0R\}}{R} \mathbf{E}_\infty(\theta, \phi) + O(R^{-2}), \quad R = |\mathbf{r}| \rightarrow \infty, \quad z > 0.$$

We asymptotically estimate the Weyl–Sommerfeld integrals involved in (7) [8], which yields to the following representation for the θ, φ -components of the far field pattern corresponding to representation (10)

$$\begin{aligned} E_{\infty,\theta}^P(\theta, \varphi) = ik_0 \sum_{m=0}^M \cos(m+1)\varphi (i \sin\theta)^m \sum_{n=1}^{N_m^0} \{ p_{nm}^0 \cos\theta [f'_n + (v_n^e - v_n \sin^2\theta) f_n] \\ + q_{nm}^0 (f'_n + v_n^h f_n) \} - ik_0 \sin\theta \sum_{n=1}^{N_m^0} r_n^0 (f'_n + v_n^h f_n), \end{aligned} \quad (11)$$

$$E_{\infty,\varphi}^P(\theta, \varphi) = -ik_0 \sum_{m=0}^M \sin(m+1)\varphi (i \sin \theta)^m \sum_{n=1}^{N_m^0} \{p_{nm}^0(f_n' + v_n^e f_n) + q_{nm}^0 \cos \theta [f_n' + (v_n^h - v_n \sin^2 \theta) f_n]\}, \quad (12)$$

where corresponding spectral functions are:

$$v_n^{e,h}(\theta, z_n) = ik_0 \cos \theta \exp\{ik_0 d \cos \theta\} A_{11}^{e,h}(k_0 \sin \theta, z_n),$$

$$v_n(\theta, z_n) = ik_0 \cos \theta \exp\{ik_0 d \cos \theta\} A_{31}(k_0 \sin \theta, z_n),$$

and

$$f_n = \exp\{-ik_0 z_n \cos \theta\}, f_n' = \exp\{ik_0 z_n \cos \theta\}.$$

So, after the unknown amplitudes of discrete sources are determined, far field pattern components (11), (12) are represented as finite linear combinations of elementary functions. This circumstance ensures economical computer analysis of the scattering characteristics in the wave zone.

3. Results and discussion

In this section we consider computer simulation results associated with conversion evanescent waves into scattered ones by a particle deposited on a metal-filmed glass prism. We analyse the differential scattering cross-section (DSC), which is given by

$$\text{DSC}(\beta_1, \theta, \varphi) = |E_{\infty,\theta}^P(\beta_1, \theta, \varphi)|^2 + |E_{\infty,\varphi}^P(\beta_1, \theta, \varphi)|^2.$$

Here $E_{\infty,\theta,\varphi}^P(\theta, \varphi)$ are the components of the far field pattern (11), (12) corresponding to the P -polarized excitation measured in μm^2 . We compute an integral response

$$R(\beta_1) = \int_{\Omega} \text{DSC}(\beta_1, \theta, \varphi) d\omega, \quad (13)$$

which represents intensity scattered in a certain solid angle $\bar{\Omega}$. The integral response is used to evaluate scattered intensity captured by lens immersed in water [4].

We examine the exciting plane wave at the wavelengths in free space $\lambda = 633$ and $\lambda = 488$ nm. Let the glass prism have the refractive index of $n_1 = 1.52$. We will assume that a particle with refractive index $n_i = 1.60$ is located in water characterized by the refractive index $n_0 = 1.33$. So, an evanescent wave appears at incident angles $\beta_1 > \beta_c$ where $\beta_c = \arcsin(n_0/n_1)$, for our case $\beta_c \approx 61.05^\circ$. We consider a plane wave propagating from prism side in this case $90^\circ > \beta_1 \geq 0^\circ$ and $\beta_{f,0}$ can be determined using the Snell's law. Recall that $\beta_1 = 0^\circ$ corresponds to a plane wave propagating normally to the prism surface.

One of the specific features of the schemes involved in express diagnosis, which is applied to detect of viruses in solutions, is the presence of metallic film on the glass prism surface. For this purpose various metals such as aluminium, copper, silver and gold can be used [4]. The film thickness varies from 10 to 100 nm. Inside a film free electrons amplify the intensity of a P -polarized evanescent wave [3]. To investigate this effect and optimise the incident field parameters and film thickness (β_1, d) we analyse the following quantity:

$$E^P(\beta_1, d) = \frac{|T^P|^2}{|T_{01}^P|^2}, \quad (14)$$

where T^P is the transmission coefficient for the metal-film prism expressed by (5) and T_{01}^P coefficient corresponds to the case $d = 0$. Quantity E^P represents the coefficient of evanescent wave amplification due to the presence of a metal film.

First, let us consider the wavelength $\lambda = 633$ nm. In this case, it has been found that silver characterized by the complex refractive index $n_f = 0.16 - 3.80j$ is the most suitable (aluminium, copper, silver and gold have been treated).

Fig. 2 demonstrates E^P versus incident angle β_1 at various values of the film thickness. Salient point of the curves corresponds to critical angle β_c . It is clear that the maximum value of the intensity enhancement is attained in the vicinity of the point $\beta_1 = 70^\circ$ and exceeds a value of 10. The dependence of E^P on film thickness d is depicted in the Fig. 3 at several incident angles. The investigation performed allows one to choose “optimal” values for (β_1, d) .

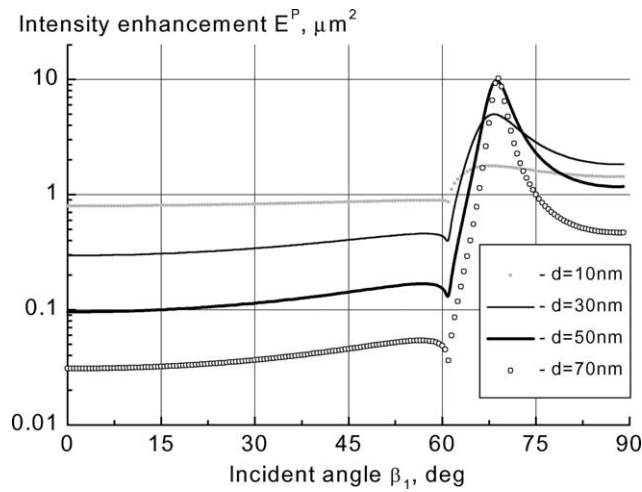


Fig. 2. Intensity enhancement E^P : (14) versus incident angle β_1 (in degrees). Four values of Ag film thickness $d = 10, 30, 50$ and 70 nm are considered. Herein after the exciting wavelength is 633 nm.

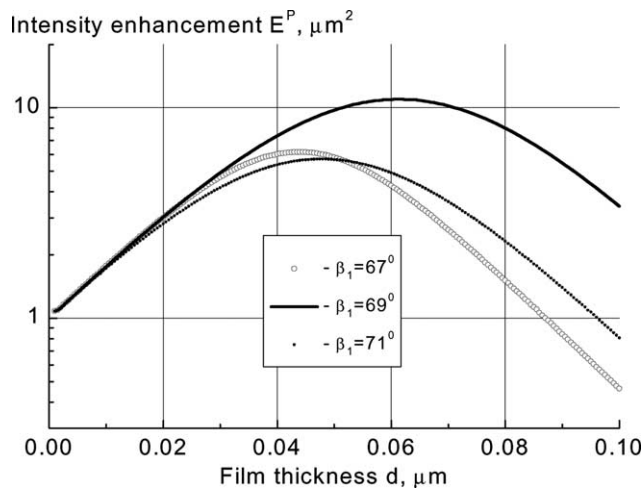


Fig. 3. Intensity enhancement E^P versus Ag film thickness (in μm). Three incident angles $\beta_1 = 67^\circ, 69^\circ$ and 71° are considered.

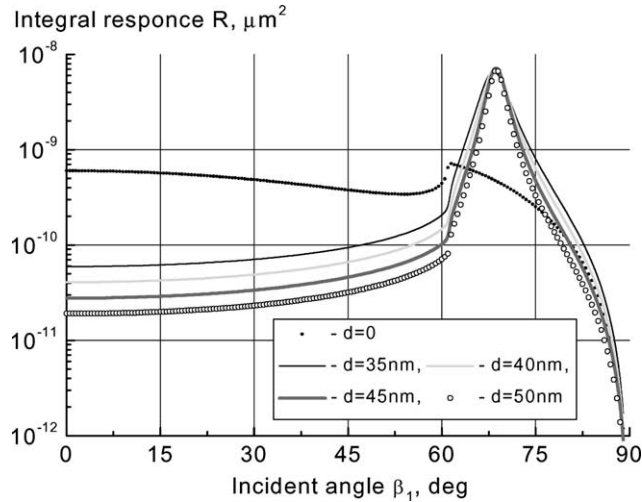


Fig. 4. Integral response R : (13) (in μm^2) versus incident angle β_1 for spherical PSL particle $D = 20$ nm. Five film thickness $d = 0$ (no film), 35, 40, 45 and 50 nm are considered.

In Fig. 4, we plot the integral response of a spherical particle of the diameter $D = 20$ nm corresponding to the solid angle $\bar{\Omega} = \{37.5^\circ \geq \theta \geq 0; 360^\circ > \varphi \geq 0^\circ\}$. It is assumed that the lens is embedded in water far from the interface [4]. These results enable us to correct the optimal values for (β_1, d) obtained at the first stage of the investigation. Let us choose a silver film of the thickness $d = 45$ nm and consider the incident angle $\beta_1 = 69^\circ$. We analyse the integral response under particle diameter variations. The corresponding results are depicted in Fig. 5. For comparison we present results obtained for the optimal values found and for a pure prism case $d = 0$. For the last case the incident angle was chosen close to the critical value to provide the maximal response (see Fig. 4). It is seen that the optimal values realise a response higher by an order of magnitude in the entire range of diameters not only for spherical particles but for prolate and oblate spheroids (the aspect ratio is 1:1.5) as well. The results for equivolume particles were compared.

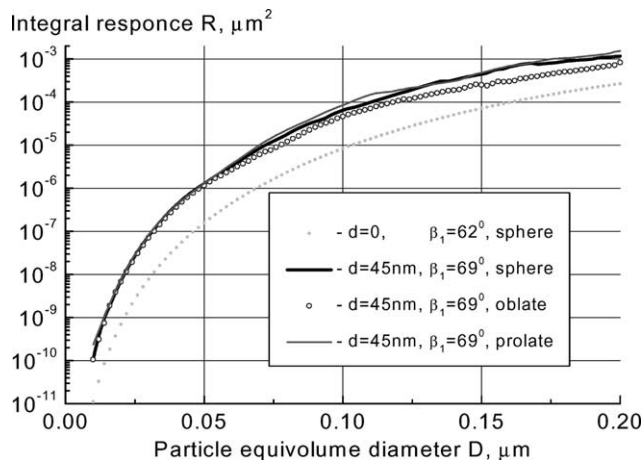


Fig. 5. Integral response versus particle equivolume diameter (in μm). Responses for $d = 0$, $\beta_1 = 62^\circ$ and $d = 45$ nm, $\beta_1 = 69^\circ$ (sphere, oblate and prolate spheroids) are considered.

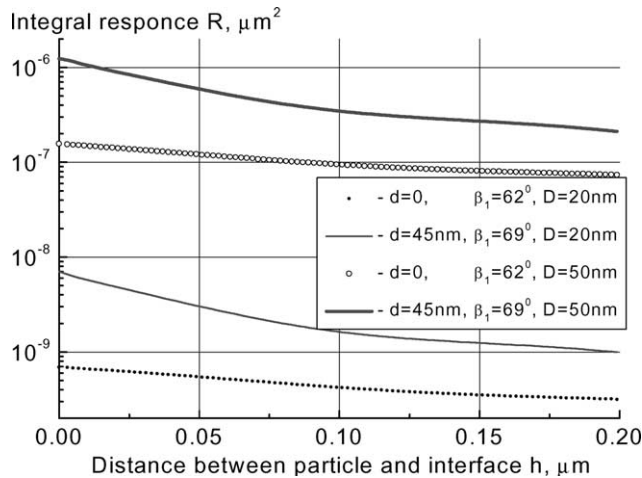


Fig. 6. Integral response versus distance between spherical particle ($D = 20$ and 50 nm) and the interface (h in μm). Responses for $d = 0$, $\beta_1 = 62^\circ$ and $d = 45$ nm, $\beta_1 = 69^\circ$ are considered.

Fig. 6 shows the integral response variation versus the distance between particle and the interface for particles with $D = 20$ and 50 nm. As before, the optimal values seem to be preferable in the entire range of distances.

Let us consider the wavelength $\lambda = 488$ nm. Similarly to the previous case, it has been found that the more suitable metal is silver with the refractive index $n_f = 0.13 - 2.82j$. Let us follow the scheme described above. First, consider the dependence of E^P on the incident angle (Fig. 7) and film thickness (Fig. 8). Note that the results resemble those obtained before. Therefore, it seems reasonable to choose the film thickness $d = 50$ nm and incident angle $\beta_1 = 78^\circ$ as a basis for the following specification. However, the subsequent analysis based on the DSM has shown that there exist other values, which realise a higher integral response (see Fig. 9). In Fig. 9 it is seen that the film thickness $d = 32$ nm and incident angle $\beta_1 = 75^\circ$ provide a

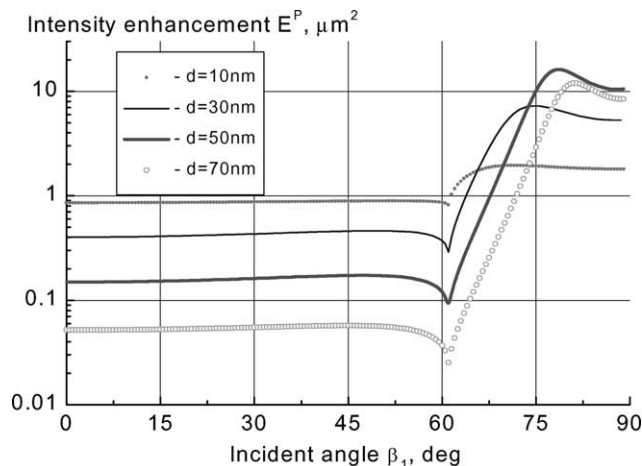


Fig. 7. Intensity enhancement E^P versus incident angle β_1 . Four Ag film thickness $d = 10, 30, 50$ and 70 nm are considered. Herein after the exciting wavelength is 488 nm.

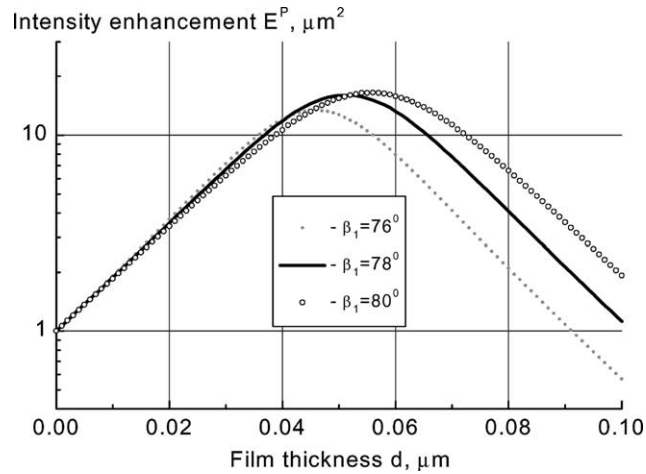


Fig. 8. Intensity enhancement E^P versus Ag film thickness. Three incident angles $\beta_1 = 76^\circ$, 78° and 80° are considered.

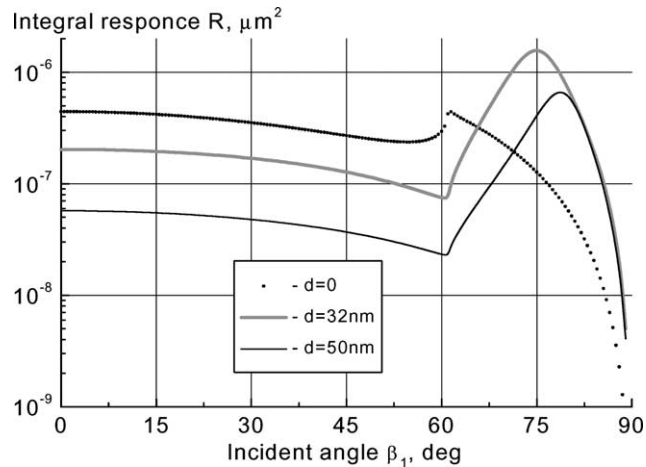


Fig. 9. Integral response R versus incident angle β_1 for spherical PSL particle $D = 50$ nm. Three values of film thickness $d = 0$, 32 and 50 nm are considered.

higher integral response. This circumstance means that interaction between the field scattered by a particle and a multi-layered interface plays a key role and must be taken into account. Fig. 10 demonstrates the integral response versus of the particle diameter. Results for a spherical particle and prolate and oblate spheroids are depicted too. It is clear that the optimal values work rather well up to the particle diameter $D = 150$ nm. In Fig. 11 the integral response corresponding to the different values of (β_1, d) versus the distance between a particle and the interface is depicted. One can see that the optimal values provide higher response up to distance of 130 nm.

4. Conclusion

Based on the discrete sources method, computer model for analysis of the evanescent waves conversion into scattered ones by a non-spherical particle located near a metal-coated glass prism has been developed.

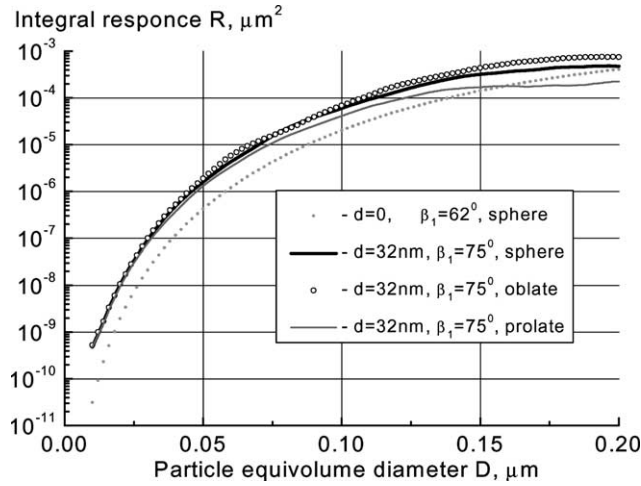


Fig. 10. Integral response versus particle equivolume diameter. Responses for $d = 0$, $\beta_1 = 62^\circ$ and $d = 32$ nm, $\beta_1 = 75^\circ$ (sphere, oblate and prolate spheroids) are considered.

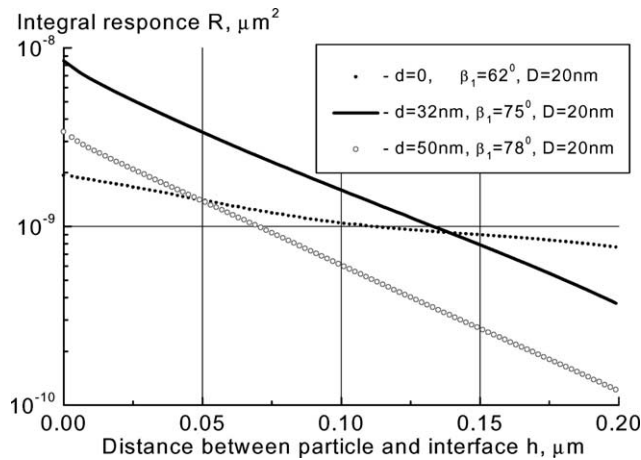


Fig. 11. Integral response versus distance between spherical particle $D = 20$ nm and the interface. Responses for $d = 0$, $\beta_1 = 62^\circ$; $d = 32$ nm, $\beta_1 = 75^\circ$ and $d = 50$ nm, $\beta_1 = 78^\circ$ are considered.

The optimal value of (β_1, d) providing the maximum lens response has been accomplished. It has been shown that the interaction between the field scattered by a particle and a multi-layered interface plays a key role and must be taken into account in the theoretical model.

Acknowledgements

We gratefully acknowledge funding of this research by Deutsche Forschungsgemeinschaft (DFG) and the Russian Foundation for Basic Research (RFBR).

References

- [1] G.S. Agarwal, *Pure Appl. Opt.* 7 (1998) 1143.
- [2] M. Ohlem, *Lasers Med. Sci.* 16 (2001) 159.
- [3] E.A. Perkins, D.J. Squirrell, *Biosens. Bioelectron.* 14 (2000) 853.
- [4] D. Ganic, X. Gan, M. Gu, *Optik* 113 (3) (2002) 135.
- [5] M. Quinten, A. Pack, R. Wannemacher, *Appl. Phys. B.* 68 (1999) 87.
- [6] A. Doicu, Yu.A. Eremin, T. Wriedt, *Comput. Phys. Commun.* 134 (2001) 1.
- [7] A. Doicu, Yu.A. Eremin, T. Wriedt, *Opt. Commun.* 190 (2001) 5.
- [8] Yu.A. Eremin, *J. Commun. Technol. Electron.* 45 (2000) 269.
- [9] W.C. Chew, *Waves and fields in inhomogeneous media*, New York, 1990.
- [10] A. Doicu, Yu.A. Eremin, T. Wriedt, *Acoustic and Electromagnetic Scattering Analysis Using Discrete Source*, Academic Press, London, 2000.